Japanese Journal of Applied Physics

The Japan Society of Applied Physics

REGULAR PAPER • OPEN ACCESS

Mid-infrared cavity ring-down spectroscopy using DFB quantum cascade laser with optical feedback for radiocarbon detection

To cite this article: Ryohei Terabayashi *et al* 2020 *Jpn. J. Appl. Phys.* **59** 092007

View the article online for updates and enhancements.

This content was downloaded from IP address 63.239.65.98 on 10/11/2020 at 18:06

OPEN ACCESS

Japanese Journal of Applied Physics **59**, 092007 (2020) **REGULAR PAPER**

https://doi.org/10.35848/1347-4065/abb20e

Mid-infrared cavity ring-down spectroscopy using DFB quantum cascade laser with optical feedback for radiocarbon detection

Ryohei Terabayashi[1*], Keisuke Saito[1], Volker Sonnenschein[1], Yuki Okuyama[1], Testuo Iguchi[1], Masahito Yamanaka[1], Norihiko Nishizawa[1], Kenji Yoshida[2], Shinichi Ninomiya[2], and Hideki Tomita[1]

[1]*Department of Engineering, Nagoya University, Nagoya, Aichi 464-8603, Japan*
[2]*Drug Development Solutions Center, Sekisui Medical Co., Ltd., Tokai, Ibaraki 319-1112, Japan*

[*]E-mail: terabayashi.ryouhei@h.mbox.nagoya-u.ac.jp

Received May 29, 2020; revised August 20, 2020; accepted August 23, 2020; published online September 7, 2020

A linewidth reduction of a distributed feedback quantum cascade laser (DFB-QCL) based on optical feedback for a mid-infrared (MIR) cavity ring down spectroscopy (CRDS) ^{14}C spectrometer is presented. A cat-eye reflector as well as a path-length enhancement by a Herriott cell were employed for a compact optical setup. The laser linewidth was evaluated by monitoring the beat frequency between the DFB-QCL and a MIR optical frequency comb (OFC). The linewidth reduction by optical feedback was clearly observed although slow frequency drifts caused by environmental changes were still visible. A low-bandwidth beat-note lock to the OFC was conducted for long-term stabilization as well as for precise frequency scanning and thereby ^{14}C measurement by MIR CRDS with optical feedback was demonstrated successfully.
© 2020 The Japan Society of Applied Physics

1. Introduction

Recent development of mid-infrared (MIR) lasers as well as MIR optics enables measurements involving fundamental absorption lines of several species of atmospheric molecules composed of hydrogen, carbon, oxide, nitrogen and sulfur.[1)] Continuous-wave cavity ringdown spectroscopy[2)] (CW-CRDS) using MIR lasers is gaining greater attention as a novel technique to analyze a variety of gas molecules or isotopologues with high sensitivity.[3–6)] Among them, radiocarbon (^{14}C) detection by CRDS proposed by Tomita et al.[7)] is expected to become a cost-effective alternative to accelerator mass spectrometry. Several groups reported their systems measuring the ν_3 band absorption line of $^{14}C^{16}O_2$ at 2209 cm^{-1},[8–13)] as well as demonstrations of ^{14}C in vivo studies in the field of drug development.[14,15)] Most of these works were performed with CW distributed feedback quantum cascade laser (DFB-QCL), a MIR light source which is commercially available and easy to handle as well. As a result, it is widely employed in MIR spectrometers for various targets, while the other MIR laser generations such as an optical parametric oscillator[16)] can produce higher output power.

The output frequency of DFB-QCL can be tuned linearly by changing the applied current to the QCL chip; the typical mode-hop-free tuning range of a few cm^{-1} can be slightly shifted by a change of the chip temperature. Generally, this is sufficient for an appropriate selection of a target absorption line, however, the linewidth of QCL becomes a serious issue due to the strict resonance condition of a high-finesse cavity used in a typical CRDS setup. In our setup, the optical cavity composed of two highly reflective mirrors (reflectivity: $R > 99.98\%$) has a finesse of above 20 000 with a free spectral range (FSR, represented by ν_{FSR}) of 336 MHz, resulting in a width of the resonance peak of less than 20 kHz. Since the typical free-running DFB-QCL linewidth is around (or just below) 1 MHz, only a small fraction of the injected photons are stored in the cavity and contribute to the CRDS signal. Such inefficient coupling between the QCL and the high-finesse cavity results in a low signal to noise ratio of the detector signal preventing us from reaching higher sensitivity.

For laser linewidth reduction or frequency stabilization for CRDS, the Pound–Drever–Hall (PDH) technique[17)] is well known, which can realize a strong active lock to an optical cavity; a representative sensitivity improvement of frequency-stabilized CRDS[18)] by PDH can be found in Refs. 19, 20. Parts per quadrillion level radiocarbon detection based on saturated absorption cavity ring-down spectrometer (SCAR) has been demonstrated with a PDH locked QCL as well.[9)] While implementing this technique is promising, it requires high speed electronics and an electro-optical modulator for high bandwidth laser phase modulation, which are cost prohibitive and whose performance characteristics are limited in MIR. Furthermore, to generate a reliable error signal, pre-stabilization may be required as feedback loop bandwidth requirements get stricter if the laser linewidth becomes large compared to the cavity resonance width.

Instead of PDH locking, passive optical feedback techniques also known as delayed self-injection locking[21,22)] can be applied to reduce the optical linewidth. In these techniques, a part of emitted photons are returned to the laser chip by an external reflection. We have previously reported successful QCL linewidth reduction via optical feedback from a "cat-eye" reflector[23)] composed of a flat gold mirror and a convex lens.[24)] Recently, a MIR optical frequency comb (OFC) is in development by our group, which enables us to perform direct frequency monitoring of the QCL as well as its linewidth measurement. In this paper, we present further results of the measurements using optical feedback QCL linewidth reduction. By employing a frequency locking technique utilizing the OFC, precise frequency scanning to acquire $^{14}CO_2$ spectrum by our MIR CRDS system with optical feedback was demonstrated as well.

2. Experimental details

2.1. General optical system

Our MIR CRDS system is designed for radiocarbon detection toward biomedical applications. Since the details of whole

Content from this work may be used under the terms of the Creative Commons Attribution 4.0 license. Any further distribution of this work must maintain attribution to the author(s) and the title of the work, journal citation and DOI.

 © 2020 The Japan Society of Applied Physics

system were presented in the previous papers,[13,25] here we only focus on the optical system: in particular, the optical feedback construction and the experimental setup for linewidth evaluation using the MIR OFC.

A simplified schematic of the experimental setup is shown in Fig. 1. The DFB-QCL (Hamamatsu Photonics, LE0833QCL) was selected for targeting the $^{14}C^{16}O_2$ absorption line at 2209.108 cm^{-1}, which is in a package including collimation lens with a typical output power of about 40 mW. For lower frequency noise, a low noise QCL current driver (Wavelength Electronics, QCL1000LAB) as well as a high-resolution temperature controller (Wavelength Electronics, PTC2.5K-CH) were installed. The QCL temperature was fixed at around 300 K for the target line. Its frequency can be linearly tuned around 2208–2210 cm^{-1} by changing the applied current in a range of 0.2 A (from 0.8 to 1.0 A). This modulation can be performed via a modulation input of the QCL driver (with DC to 3 MHz bandwidth). The main beam reached the CRDS optical cavity (reflectivity: $R > 99.98\%$, length: $L = 44.5$ cm) after passing through an optical isolator, an acoustic optical modulator and a mode-matching telescope. One of the cavity mirrors was mounted with a ring piezo actuator to modulate the cavity length. Behind the optical isolator, a portion of the laser light was picked up by a wedged CaF_2 window for a wavelength calibration by a solid silicon etalon (Lightmachinery, $\nu_{FSR} =$ 527 MHz) and a N_2O reference cell (Wavelength References). To measure their light transmission, InAsSb photodiodes (Hamamatsu Photonics) operated at room temperature were used with slow transimpedance amplifiers (10^7 V A^{-1}, 2 kHz bandwidth). The whole optical layout was arranged on a 60 cm square aluminum breadboard.

2.2. Optical feedback system

In front of the isolator, a 50/50 CaF_2 beam splitter was introduced to the QCL optical system for optical feedback. In addition to the "cat eye" reflector[24] (feedback path-length: 16 cm), a multi-path reflector consisting of two concave mirrors with off-axis holes as typically employed for Herriott cells[26] was implemented to drastically increase the feedback path length, while keeping a compact configuration. An effective path-length between the two mirrors of 273 cm was estimated by counting the number of reflections using a visible alignment laser and multiplying by the mirror spacing of 13 cm. Combined with the distance to the final gold mirror, a total feedback path length of 350 cm was reached. The compact size of this optical feedback system helps with the implementation of a stabilized enclosure, which should lead to higher frequency stability as will be discussed in the next section. The feedback system was not stabilized yet, though the main optical setup was covered by an acrylic box, which provided a weak isolation from the environment. A flip mirror mount allowed for convenient switching between the two paths and feedback could be turned on/off with a beam shutter. A piezo actuator was installed on each end-mirror respectively, to adjust the feedback path-length.

2.3. Beat-note detection setup

Another small portion of the QCL beam was picked up for the MIR-OFC beat note setup. The MIR-OFC was developed by our colleagues:[27] a carrier-envelope offset should be zero as it is generated via difference frequency generation with the repetition frequency (f_{rep}) of 191 MHz. Both lasers were coupled into a single-mode fiber to establish a good spatial overlap. Unwanted parts of the MIR-OFC spectrum were filtered by an optical grating in combination with a slit and sent to a fast MCT detector (VIGO systems, PVI-4TE-5, 200 MHz bandwidth), whose signal was connected to a RF analyzer (Signal Hound, BB60C) to acquire the beat-note spectrum. This system enables evaluation of the QCL linewidth as well as accurate frequency calibration. We already demonstrated QCL frequency locking to the MIR-OFC including a successful ^{14}C measurement, which is under preparation to be published elsewhere in the near future for more details.

3. Results and discussion

3.1. Feedback effect and linewidth reduction

To check the feedback effect from the newly installed multi-path reflector, the QCL current was scanned and the Si etalon signal was monitored. As shown in Fig. 2(a), a step-like behavior of the signal was visible only with feedback, while the free-running QCL signal changed smoothly. This is a clear evidence of feedback, with the steps caused by mode-hopping of the external cavity coupled to the QCL during the current scan. Since this mode-hopping was observed 11–12 times within one period of the Si etalon, the FSR of the feedback cavity was estimated to be around 46 ± 2 MHz. This

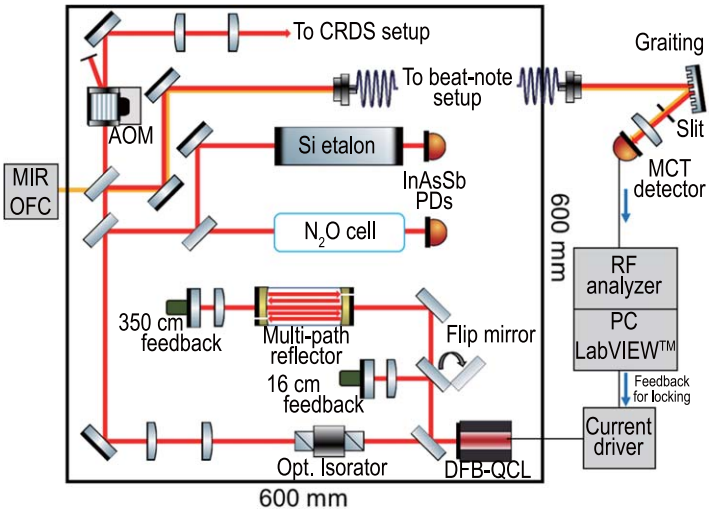

Fig. 1. (Color online) Overview of the experimental setup. The components with no indication are either gold mirrors, optical lenses, or beam splitters.

© 2020 The Japan Society of Applied Physics

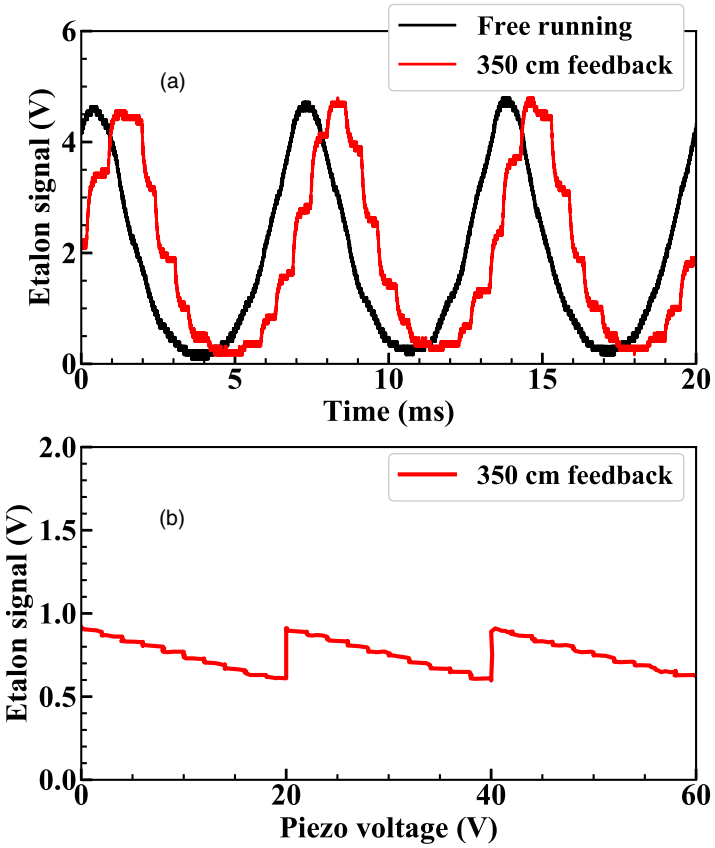

Fig. 2. (Color online) Si etalon transmission signals taken by QCL current scanning (a), or by modulating feedback path-length via the piezo actuator (b). The repeated jumps were caused by mode-hopping.

value matched well to the feedback path-length of 350 cm assuming $\nu_{FSR} = c/2\,L$.

Instead of scanning the QCL current, feedback path-length modulation was tested by applying a sawtooth ramp voltage (0–60 V, 5 Hz) to the piezo. Figure 2(b) shows the Si etalon signal depending on the piezo voltage. A nearly linear frequency change could be observed between successive jumps in frequency (mode-hopping). To increase the mode-hop-free tuning range, synchronization between QCL current and path-length modulation is necessary. While this may be realized in the same way as used in external cavity diode lasers,[28] environmental instability of the long feedback path may require frequent re-optimization of parameters. Another approach is to increase the effective FSR of the feedback cavity using dual cavity optical feedback.[29] This approach was attempted as well, however we found it difficult to balance the feedback strength of such a dual cavity properly in our MIR free-space setup and were not able to replicate the increased FSR. Another option is to use a shorter path-length and reduce environmental influences by passive isolation. However, a shorter path-length was found to have weaker effects on the spectral linewidth as will be shown in the next section.

Since our MIR-OFC is still under development, its linewidth was not evaluated except for a long term f_{rep} stability of less than 10 Hz over 30 min, using a slow stabilization loop with a time constant of around 250 ms. This means each comb mode has an instability of a few MHz over long timescales. Although the short-term stability (or the linewidth) would be much lower, it is emphasized that this MIR-OFC instability partially contributed to the results shown in the following. Despite that, the linewidth reduction by optical feedback was evidently observed in the RF beat spectra. A typical beat spectrum is shown in Fig. 3(a). The sweep frequency range of 100–200 MHz covered the beat signal located in $f_{rep}/2-f_{rep}$ region with 100 kHz resolution bandwidth. A single sweep took around 10 ms. The linewidth and the amplitude of the beat was improved by optical feedback, which were estimated from Gaussian fits. A histogram of the 3 dB linewidth is displayed in Fig. 3(b). The linewidth reduction was observed for either of the feedback paths and the longer distance resulted in a stronger effect. The beat spectral linewidth indicates an upper limit for the short-term laser linewidth, as the measurement was affected by acoustic noise and frequency drifts during the sweep of the RF analyzer. Thus, a result with a better isolated system should show a greater effect of the long-path feedback. Figure 3(c) shows the result of beat position tracing for 10 min. As f_{rep} of the MIR-OFC was stabilized at 191 MHz, the slow drifts of the beat position can be attributed mainly to QCL frequency fluctuations. The large periodic oscillations in "16 cm feedback" were caused by environmental changes such as temperature of air conditioner and water chiller, whose cycling period observed by room temperature monitoring was a few minutes. Similar long-term drift was observed for the long and short feedback path, however larger short-term fluctuations are noticeable for the short path. This may be due to localized temperature fluctuations as this path was close to a cable entrance hole in the acrylic box. Periodic fluctuations were visible in "free-running" mode as well, which is most likely caused by the temperature drifts of the QCL chip, affected by the water chiller for its heat sink. To reduce these

© 2020 The Japan Society of Applied Physics

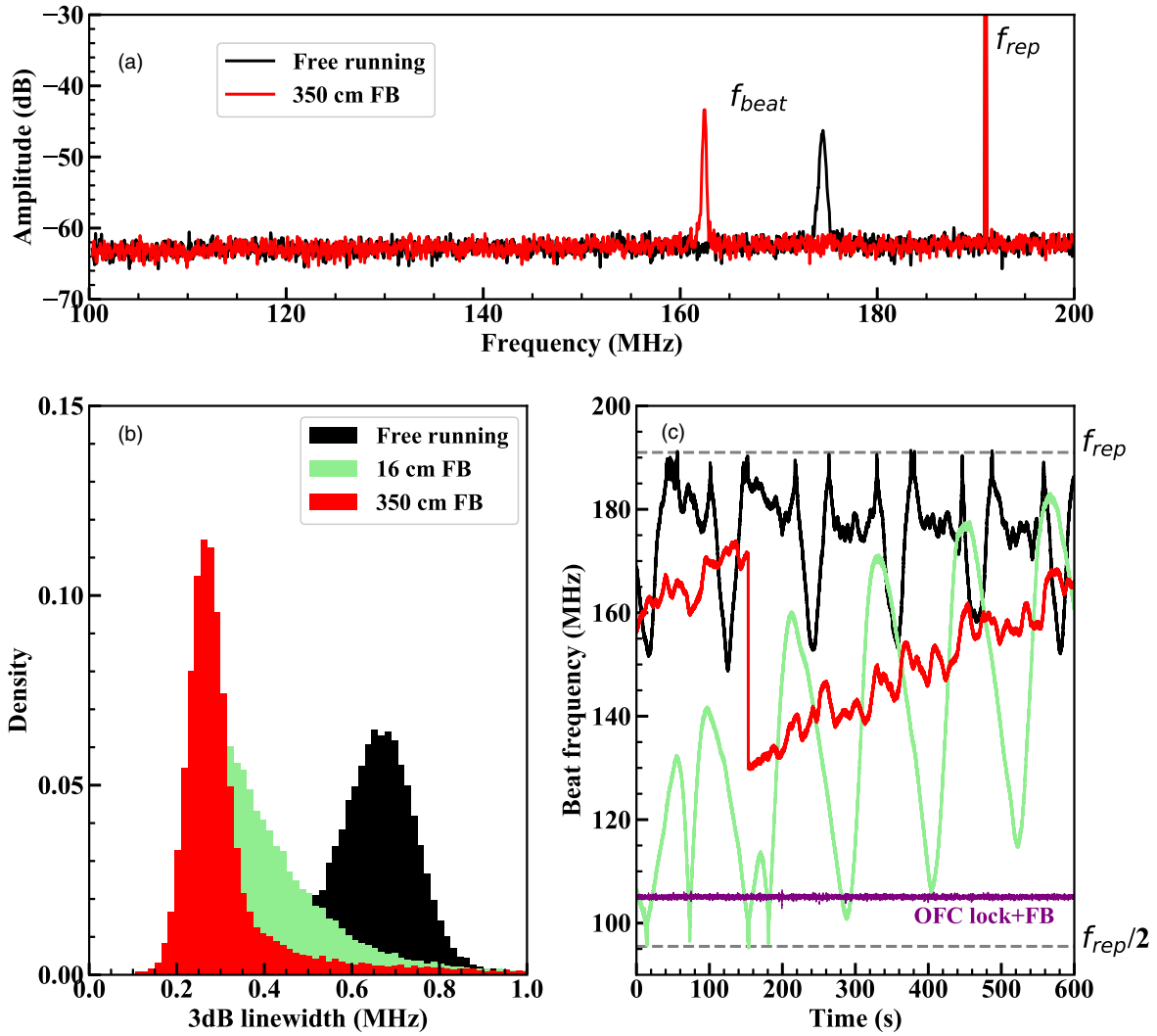

Fig. 3. (Color online) QCL frequency monitoring with MIR-OFC beat-note measurements: raw spectra acquired by the RF analyzer (a), histograms of 3 dB linewidth of the beat spectra (b), and peak tracing results of the beat for 600 s (same color code) (c). The beat frequency varied between $f_{rep}/2$ and f_{rep} and returned when reaching the limits, with the opposite polarity for the frequency change direction. "OFC lock+FB" in (c) reveals the result of frequency stabilization by MIR-OFC locking, with a fixed setpoint of 105 MHz.

slow drifts with optical feedback, the whole assembly of the optical system needs to be covered with a temperature stabilized box for better isolation from atmosphere, which is now under construction. The CRDS cavity transmission improved: higher signal intensity and lower fluctuations resulting in a smaller fitting error of the ring-down rate. Its noise spectral density (periodogram) improved as well, which was shown in our previous report[24]: a noise reduction up to 30 dB was observed above 50 kHz although the noise level at relatively low frequencies was increased. The results denoted with "OFC locked feedback" in Fig. 3(c) are discussed in the next section.

3.2. Demonstration of CRDS measurement

Because the mode-hop-free tuning range with the 350 cm path length was insufficient to cover the $^{14}CO_2$ absorption region, the shorter 16 cm path (calculated $\nu_{FSR} \sim 1$ GHz) was chosen for the CRDS demonstration.

Usually the Si etalon and N_2O cell was used to calibrate the QCL frequency (x-axis) of acquired absorption spectra, but the number of N_2O peaks within the tuning range of the present optical feedback was not sufficient for accurate calibration. Besides, the mid/long term instability of the center frequency was also a large issue. Instead, MIR-OFC beat-note locking was utilized to perform calibration of $^{14}CO_2$ spectrum measurements with the present feedback setup. The usual calibration setup as discussed above should become possible after implementing a stabilized enclosure and synchronized QCL current tuning.

The locking procedure was as follows. First, the QCL current was fixed close to the target frequency region and the beat frequency was monitored by real-time fitting in a LabVIEW program. This program was used for operation of the RF analyzer and a digital to analog converter for control of piezo voltage and QCL current modulation. A PID control loop in the program then varied the piezo voltage to keep the beat position constant at a given setpoint value. The QCL frequency was scanned by a step by step change of the setpoint. This was sufficient for the purpose of combining optical feedback linewidth reduction with frequency scanning. As shown in Fig. 3(c), the beat frequency was well stabilized by this locking with a rms frequency fluctuation below 220 kHz.

To investigate the effect of optical feedback to CRDS sensitivity, the Allan deviation (AD)[30] was calculated for the datasets of the ringdown signals obtained at fixed QCL current (Fig. 4). The ringdown signals were obtained at an

© 2020 The Japan Society of Applied Physics

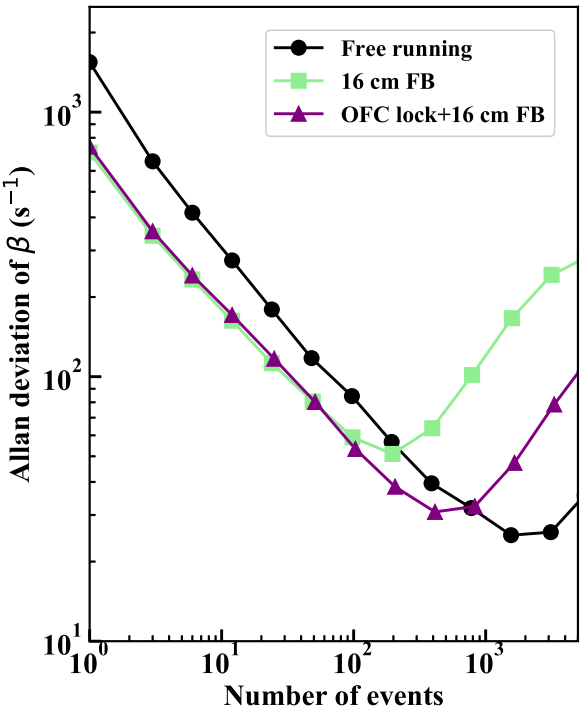

Fig. 4. (Color online) Comparison of Allan deviations. These measurements were performed at fixed QCL current, however, the actual QCL frequency might slightly differ between each measurement because of optical feedback.

event rate of around 200 signals s^{-1} in each case, as determined by the cavity piezo scanning speed. However, with optical feedback, the coupling to the cavity is more efficient so that the higher transmission signal was observed so that the AD decreased by half with feedback for small averaging time. For high sample throughput applications, this means that sample measurement time can be reduced by a factor of 4 while keeping the same sensitivity. The time to reach the minimum AD became shorter. The OFC locking enables longer averaging with optical feedback as it removes the laser frequency drift, although the minimum value was close to "free-running. This shows that other drifts, in particular the systematic error due to an etalon effect still limits our long-averaging performance. This effect takes the form of a periodic oscillation in the background and depends on drifts in pressure and temperature in the experimental room as well and so is not repeatable from one measurement to another. In addition, the specific set point of the QCL frequency might slightly differ between each measurement because of the frequency shift induced by optical feedback. Due to these factors, a fair comparison of the minimum achievable AD as well as the time to reach the minimum is difficult. Attempts to cancel out etalon oscillations were reported in our previous works,[13,31] which is expected to improve comparisons by suppressing the etalon effect.

Finally, a ^{14}C measurement was conducted with optical feedback in combination with OFC locking. The sample contained an activity of 8 Bq of ^{14}C labeled glucose mixed with normal glucose and was prepared with a high isotope ratio ^{14}C/^{12}C of 1.0×10^{-8} for a first demonstration. Figure 5 shows the obtained spectrum fitted by the line-by-line calculation with the HAPI package.[1,32] Total pressure and gas cell temperature was 15 Torr, 291 K respectively. Since no mode-hopping was observed in the result of beat frequency monitoring, linear frequency scanning with optical

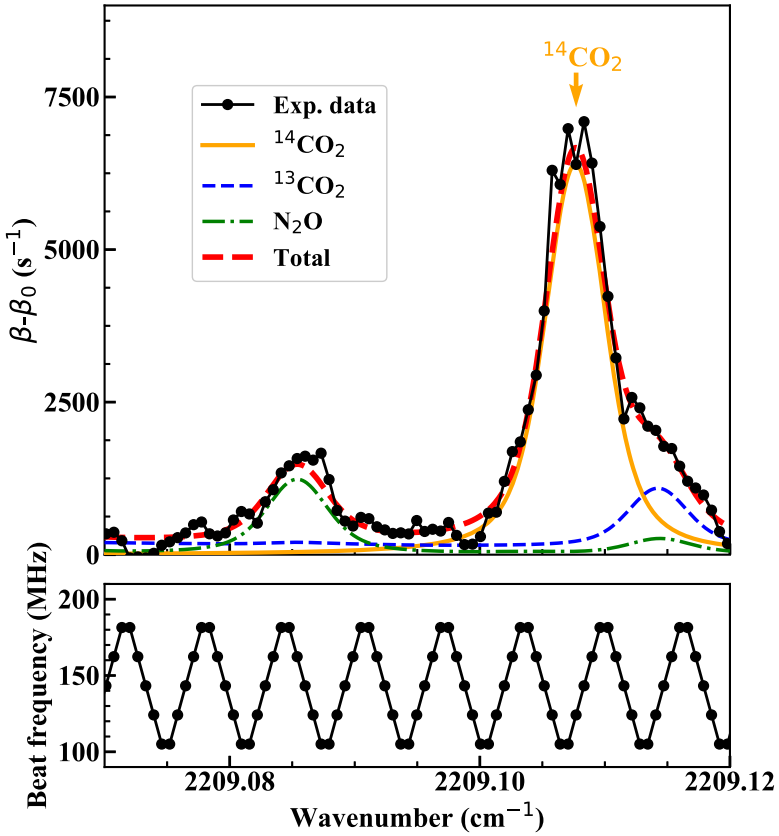

Fig. 5. (Color online) CRDS spectrum of the $^{14}CO_2$ with the fitting results using Voigt profile: estimated ^{14}C/^{12}C isotope ratio was 0.9×10^{-8}. The QCL frequency was scanned once by a step by step modulation of the setpoint of the beat frequency. The beat frequency is shown below the spectrum.

© 2020 The Japan Society of Applied Physics

feedback for the ^{14}C-CRDS measurement was successfully demonstrated, though the tuning range was still insufficient for precise quantitative evaluations of impurities such as N_2O.

4. Summary and outlook

A simple optical feedback technique for QCL was presented for our cavity ring-down ^{14}C spectrometer in the MIR region. This technique is expected to reduce the spectral linewidth effectively with lower cost compared to PDH locking. The frequency monitoring/locking system with MIR-OFC was implemented and thereby the linewidth reduction by optical feedback was clearly demonstrated. The longer feedback path utilizing a multi-path reflector revealed stronger linewidth reduction, though its mode-hop-free tuning range was insufficient for the ^{14}C measurement. A sensitivity evaluation was performed as well, calculating the AD for the ring-down rate. The noise level with short averaging time was decreased by the linewidth reduction, however, there was no significant improvement of the minimum value after long averaging even when eliminating the frequency drift by MIR-OFC locking. This is due to other factors limiting the sensitivity, such as an etalon effect. By scanning and controlling the feedback path length, a ^{14}C measurement was successfully demonstrated with MIR-OFC locking.

The present optical feedback system has some issues such as a limited tuning range and long-term frequency instability. For further improvement, a temperature stabilized sound-proof enclosure and current synchronized scanning will be implemented. This should allow us to circumvent the reliance of the system on the MIR-OFC for frequency calibration. Even though the OFC is a convenient and precise calibration tool, it is relatively expensive and not always available. In a parallel development we will also attempt a frequency filtered optical feedback technique. This technique should allow for an even greater reduction in linewidth but requires additional optics and has increased complexity.

Acknowledgments

This work was partially supported by JSPS KAKENHI: Grant-in-Aid for Scientific Research (B) 18H03469, for Early-Career Scientists 20K15205, and JST PRESTO Grant Number JPMJPR19G7, Japan.

ORCID iDs

Ryohei Terabayashi https://orcid.org/0000-0001-9285-4158
Volker Sonnenschein https://orcid.org/0000-0001-9513-8069
Masahito Yamanaka https://orcid.org/0000-0002-5862-177X
Norihiko Nishizawa https://orcid.org/0000-0002-6520-3736
Hideki Tomita https://orcid.org/0000-0002-5192-6001

1) I. E. Gordon et al., J. Quant. Spectrosc. Radiat. Transf. **203**, 3 (2017).
2) D. Romanini, A. A. Kachanov, N. Sadeghi, and F. Stoeckel, Chem. Phys. Lett. **264**, 316 (1997).
3) D. A. Long, A. J. Fleisher, Q. Liu, and J. T. Hodges, Opt. Lett. **41**, 1612 (2016).
4) A. Maity, M. Pal, G. D. Banik, S. Maithani, and M. Pradhan, Laser Phys. Lett. **14**, 115701 (2017).
5) G. D. Banik, S. Som, A. Maity, M. Pal, S. Maithani, S. Mandal, and M. Pradhan, Anal. Methods **9**, 2315 (2017).
6) S. Maithani, S. Mandal, A. Maity, M. Pal, and M. Pradhan, Analyst **143**, 2109 (2018).
7) H. Tomita, K. Watanabe, Y. Takiguchi, J. Kawarabayashi, and T. Iguchi, J. Power Energy Syst. **2**, 221 (2008).
8) I. Galli, S. Bartalini, P. Cancio, P. De Natale, D. Mazzotti, G. Giusfredi, M. E. Fedi, and P. A. Mandò, Radiocarbon **55**, 213 (2013).
9) I. Galli, S. Bartalini, M. Barucci, P. Cancio, F. Cappelli, G. Giusfredi, D. Mazzotti, N. Akikusa, and P. De Natale, Optica **3**, 385 (2016).
10) G. Genoud, J. Lehmuskoski, S. Bell, V. Palonen, M. Oinonen, M. L. Koskinen-Soivi, and M. Reinikainen, Anal. Chem. **91**, 12315 (2019).
11) A. D. McCartt, T. Ognibene, G. Bench, and K. Turteltaub, Nucl. Instrum. Methods Phys. Res. Sect. B **361**, 277 (2015).
12) A. J. Fleisher, D. A. Long, Q. Liu, L. Gameson, and J. T. Hodges, J. Phys. Chem. Lett. **8**, 4550 (2017).
13) V. Sonnenschein et al., J. Appl. Phys. **124**, 033101 (2018).
14) N. A. Kratochwil, S. R. Dueker, D. Muri, C. Senn, H. J. Yoon, B. Y. Yu, G. H. Lee, F. Dong, and M. B. Otteneder, PLoS One **13**, 1 (2018).
15) A. Kim, S. R. Dueker, F. Dong, A. F. Roffel, S. W. Lee, and H. Lee, Bioanalysis **12**, 87 (2020).
16) M. Vainio and L. Halonen, Phys. Chem. Chem. Phys. **18**, 4266 (2016).
17) R. W. P. Drever, J. L. Hall, F. V. Kowalski, J. Hough, G. M. Ford, A. J. Munley, and H. Ward, Appl. Phys. B **31**, 97 (1983).
18) J. T. Hodges and R. Ciurylo, Rev. Sci. Instrum. **76**, 023112 (2005).
19) A. Cygan, D. Lisak, P. Masowski, K. Bielska, S. Wjtewicz, J. Domysawska, R. S. Trawiski, R. Ciuryo, H. Abe, and J. T. Hodges, Rev. Sci. Instrum. **82**, 063107 (2011).
20) A. Cygan, D. Lisak, S. Wójtewicz, J. Domysławska, J. T. Hodges, R. S. Trawiński, and R. Ciuryło, Phys. Rev. A **85**, 022508 (2012).
21) R. A. Cendejas, M. C. Phillips, T. L. Myers, and M. S. Taubman, Opt. Express **18**, 26037 (2010).
22) D. Brunner, R. Luna, A. Delhom, I. Latorre, X. Porte, and I. Fischer, Opt. Lett. **42**, 163 (2017).
23) R. Beer and D. Marjaniemi, Appl. Opt. **5**, 1191 (1966).
24) R. Terabayashi et al., Hyperfine Interact. **238**, 10 (2017).
25) R. Terabayashi et al., Radioisotopes **67**, 85 (2018) [in Japanese].
26) D. R. Herriott and H. J. Schulte, Appl. Opt. **4**, 883 (1965).
27) L. Jin, V. Sonnenschein, M. Yamanaka, H. Tomita, T. Iguchi, A. Sato, K. Nozawa, K. Yoshida, S. I. Ninomiya, and N. Nishizawa, IEEE J. Sel. Top. Quantum Electron. **24**, 0900907 (2018).
28) C. Petridis, I. D. Lindsay, D. J. M. Stothard, and M. Ebrahimzadeh, Rev. Sci. Instrum. **72**, 3811 (2001).
29) S. Huang, T. Zhu, G. Yin, T. Lan, F. Li, L. Huang, and M. Liu, Sci. Rep. **7**, 1185 (2017).
30) D. W. Allan, IEEE Trans. Ultrason. Ferroelectr. Freq. Control **34**, 647 (1987).
31) R. Terabayashi et al., JPS Conf. Proc. **24**, 011024 (2019).
32) R. V. Kochanov, I. E. Gordon, L. S. Rothman, P. Wcisło, C. Hill, and J. S. Wilzewski, J. Quant. Spectrosc. Radiat. Transf. **177**, 15 (2016).

© 2020 The Japan Society of Applied Physics